

K. KOWALCZYK-GAJEWSKA*, R. B. PEĆCHERSKI*

PHENOMENOLOGICAL DESCRIPTION OF THE EFFECT OF MICRO-SHEAR BANDING IN MICROMECHANICAL MODELLING OF POLYCRYSTAL PLASTICITY

FENOMENOLOGICZNY OPIS EFEKTU MIKROPASM ŚCINANIA W MIKROMECHANICZNYM MODELOWANIU PLASTYCZNOŚCI POLIKRYSTAŁÓW

The rigid-plastic crystal plasticity model accounting for the effect of micro-shear banding mechanism on the reduction of the global strain hardening rate is presented. The instantaneous contribution of micro-shear bands in the rate of plastic deformation is described by means of the constitutive function f_{MS} that depends on the type of strain path specified by the current direction of strain rate tensor. The capabilities of the model are explored by studying the strain-stress behavior of polycrystalline material together with the crystallographic texture evolution in the polycrystalline element.

Keywords: A. Crystallographic texture, B. Anisotropic material, B. Crystal plasticity, B. Polycrystalline material, B. Micro-shear banding

Przedstawiono sztywno-plastyczny model plastyczności kryształów uwzględniający wpływ mikropasm ścinania na redukcję globalnego modułu umocnienia. Chwilowy udział mikro-pasm ścinania w prędkości deformacji plastycznej został opisany poprzez dodatkową konstytutywną funkcję f_{MS} , która zależy od schematu odkształcenia zdefiniowanego przez aktualny kierunek tensora prędkości odkształceń. Zbadano możliwości proponowanego modelu mikromechanicznego w ramach analizy odpowiedzi materiału polikrystalicznego z uwzględnieniem rozwoju tekstury krystalograficznej.

1. Introduction

1.1. The state of the art

In early works of cyclic plasticity it was observed that the change of strain path in the stress-strain cycles of large amplitude imposed on the cold-worked specimens of copper, steel and aluminum alloy produces cyclic softening (Dugdale, 1959). It was also reported by Coffin (1960) that the length of the specimen increases during cyclic loading while subjected to combined axial tension and cyclic torsion. The search for, the suggested in (Coffin, 1960), possible applications of controlled cyclic torsion for the reduction in load during drawing and extrusion processes was presented in (Kong et al., 2001). It appears, however, that the problem is far to be solved and that the understanding of the process with cyclic strain path change requires deeper experimental and theoretical studies. Independently, the effects of the change of strain path on the reduction of load in elementary tests of tension and compression as well as in the metal shaping operations of drawing, extension,

rolling and forging have been studied for two decades by Korbel and Bochniak with coworkers (Embury et al. (1984); Korbel et al. (1986); Korbel and Martin (1988); Korbel and Bochniak (2004)). The systematic experimental investigations related with microstructural analysis and physical interpretation of the phenomenon led to the conjecture that shear banding is the basic mechanism responsible for the plastic softening during the change of strain path. Also according to the experimental results described in (Anand and Kalidindi, 1994; Mohammed et al., 2007) the reduction of strain hardening is more pronounced for plane strain compression (channel die test) than for simple compression. In (Anand, 2004) it is reported that initiation of shear banding mechanism in plane strain compression was observed between the true strain level -0.21 and -0.52 and the intensity of the micro-shear bands continued to increase as deformation progresses. The strong reduction of strain hardening was observed in this range of strain in the case of compression strain-stress curves. As it was stressed in (Mróz and Pecherski, 2004), to make the new shaping operations

* INSTITUTE OF FUNDAMENTAL TECHNOLOGICAL RESEARCH OF THE POLISH ACADEMY OF SCIENCES, 02-106 WARSZAWA, 5B PAWIŃSKIEGO STR., POLAND

more efficient and suitable for industrial implementations one needs to optimize the considered forming process. This requires modelling and simulating the process numerically. To accomplish this task, the adequate constitutive description of material behavior during forming operations with the cyclic loading scheme is necessary. However, proper understanding of the phenomenon of material softening during plastic flow conditioned by cyclic loading with a particular amplitude and frequency remains an unsolved and challenging problem. In (Mróz et al., 2006) phenomenological model of the process of simple tension or compression of a cylindrical tube with imposed cyclic torsional deformation was analyzed. The material response was assumed to be rigid-perfectly plastic or elastic-perfectly plastic and analytical solutions have been provided for the steady cyclic responses as well as the effect of amplitude and frequency has been demonstrated. Our aim is to study this problem from the point of view of micromechanical modelling of metals with an attempt of providing a new description of the effects of shear banding on plastic hardening and the evolution of texture.

1.2. Experimental motivation

In our study, the term micro-shear band is understood as a long and very thin, ca. $0.1 \mu\text{m}$, sheet-like region of concentrated and intensive plastic shear crossing grain boundaries without deviation. Metallographic observation reveal that in heavily deformed metals, or even at small strains preceded by controlled change of deformation path, a multi-scale hierarchy of shear localization modes replaces the multiple slip or twinning (Pecherski, 1992, 1998b).

The first microscopic observation of shear bands on the lateral surface of the specimens of Cu-20Ni alloy subjected to 50% rolling were reported by Adcock in 1922. The further observations of microscopic and macroscopic shear band formation in different metals and alloys were discussed in (Sevillano et al., 1981). The papers of Embury et al. (1984) and Hatherly and Malin (1984) as well as Korbel et al. (1986) and Harren et al. (1988) provide many experimental results, obtained with the application of different techniques for different materials, which can give information on the mechanisms of shear banding process (cf. (Pecherski, 1992, 1998b) for more detailed discussion of this issue). Usually the following terminology is used (Korbel and Martin, 1988; Pecherski, 1992):

Micro-shear band is a long and very thin sheet-like region of concentrated plastic shear crossing grain boundaries without deviation and forming a definite pattern in relation to the principal direction of strain. It bears very

large strains and lies in a position that is not parallel with the particular slip plane of crystallites it intersects. According to the discussion in (Pecherski, 1998b), the clusters of micro-shear bands, produced for instance in rolling, form the planar structures, which are usually inclined by about $\pm 35^\circ$ to the rolling plane and are orthogonal to the specimen lateral face. There can be, however, considerable deviations from this value within 15° to 50° range. It is worthy to stress that the problem of specifying the angle is complicated by the difficulty of distinguishing the most recently formed micro-shear bands from those that were formed earlier and subsequently rotated towards the rolling plane (Hatherly and Malin, 1984). As it was emphasized in (Hatherly and Malin, 1984) and (Duggan et al., 1978) as well as (Pecherski, 1992) a particular micro-shear band operates only once and develops rapidly to its full extent. The micro-shear bands, once formed, do not contribute further to the increment of plastic deformation. It appears then that the successive generations of active micro-shear bands competing with the mechanisms of crystallographic slip and/or twinning contribute to the process of plastic flow. In (Yeung and Duggan, 1987) the question of the contribution of micro-shear bands on the example of 70/30 brass slab was studied. Applying the geometrical model of shear banding developed in (Sevillano et al., 1981) and introducing the fraction of the plastic deformation increment carried by active micro-shear bands the authors have found experimentally that this fraction changes very irregularly in deformation and in different location along the specimen. The mean value of the fraction parameter was reported between 0.6 and 0.8.

1.3. The new description of the effect of micro-shear banding

The macroscopic behavior of a polycrystal is analyzed, within the framework of continuum micromechanics, by modelling first the deformation mechanisms: crystallographic slip and micro-shear banding at the level of a single grain and performing then the micro-macro transition. The rigid plastic model of a single grain accounting for the influence of micro-shear banding on the reduction of the global hardening rate is proposed. The apparently “rough” description of the influence of shear banding on plastic hardening, in fact takes also into account the effect of the strain path change.

The novelty of our approach is that we consider the micro-shear banding as an additional mechanism of plastic deformation and apply the additive decomposition of the macroscopic measure of velocity gradient produced in the course of elastic-plastic deformation according to the contribution of dislocation mediated crystallograph-

ic slip on the one hand and micro-shear banding on the other hand. This idea has been developed in the series of papers, in particular the derivation of the mentioned additive decomposition is presented in (Pecherski, 1997, 1998a).

In the presented model **the contribution of micro-shear bands in the rate of plastic deformation is specified by the phenomenological function f_{MS}** – a sigmoid function of equivalent plastic strain and invariants describing the rate of change of deformation path (Kowalczyk-Gajewska et al., 2005). In the present paper **we focus on the simplified model in which both parts of rate of plastic deformation tensor are associated to the regularized Schmid law**. Special attention is paid to the predicted strain-stress response of the polycrystalline material in which the reduction of the global hardening rate is observed when the role of micro-shear banding in rate of plastic deformation increases. This reduction depends on the type of current deformation path. It is due to applied formulation in which **hardening occurs only as a result of a crystallographic slip (motion of dislocation)**. The important part of a paper is the identification of the model parameters and the verification of predictions involving the texture evolution and the material response by comparison with experimental results reported in (Anand, 2004; Kalidindi and Anand, 1994).

2. The constitutive modelling

2.1. Kinematics

The rigid-plastic model is considered. In order to study the texture development as well as the polycrystalline behavior for the advanced plastic deformation process the large strain formulation of the crystal plasticity theory has to be applied (Asaro, 1983). We consider behavior of a single crystal as a single grain embedded in a polycrystalline aggregate. The multiplicative decomposition of the total deformation gradient \mathbf{F} into the elastic part and the plastic part \mathbf{F}^p is used. The assumption is made that the elastic stretches are negligible comparing to the analyzed plastic strains so that the elastic part is restricted to the rigid rotation \mathbf{R}^* . It results in the additive decomposition of the the velocity gradient $\mathbf{L} = \dot{\mathbf{F}}\mathbf{F}^{-1}$ into the elastic spin $\mathbf{\Omega}^*$, the plastic spin $\mathbf{\Omega}^p$ and the rate of plastic deformation tensor \mathbf{D}^p . In crystal plasticity theories it is customary to assume that during the elastic regime the geometry of crystallographic lattice and the material undergo the same deformation while plastic deformation does not disturb the lattice geometry (Anand and Kothari, 1996). Therefore, the reorientation of the local crystallographic frame is described by the elastic spin.

One of the main assumptions of this paper, based on the derivation in (Pecherski, 1997), is that the plastic part \mathbf{L}^p of the total velocity gradient can be decomposed into two parts

$$\mathbf{L}^p = \mathbf{L}_{slip}^p + \mathbf{L}_{MS}^p, \quad (2.1)$$

where \mathbf{L}_{slip}^p is connected with the crystallographic slip mechanism of plastic deformation and \mathbf{L}_{MS}^p with micro-shear bands, which developed in certain volume of polycrystalline aggregate. \mathbf{L}_{slip}^p can be described as a sum of shearing on the active slip systems

$$\mathbf{L}_{slip}^p = \sum_{r=1}^M \dot{\gamma}^r \mathbf{m}^r \otimes \mathbf{n}^r, \quad (2.2)$$

where $\dot{\gamma}^r$ is the rate of shearing on the slip system r and a pair $\{\mathbf{m}^r; \mathbf{n}^r\}$ defines the slip system: \mathbf{n}^r being a unit normal to the crystallographic slip plane and \mathbf{m}^r – a unit crystallographic slip direction. The number M and the type of slip systems depend on the lattice type. In this paper the identification of the model parameters and numerical simulations are performed for the f.c.c. Cu crystals with 12 slip systems $\{111\} \langle 110 \rangle$. Due to hypothesis (2.1) analogical decompositions are true for symmetric and skewsymmetric parts of \mathbf{L}^p that is the strain rate tensor \mathbf{D}^p and the plastic spin tensor $\mathbf{\Omega}^p$. Let us define the ratios:

$$f_{slip/MS} = \frac{\|\mathbf{D}_{slip/MS}^p\|}{\|\mathbf{D}^p\|}, \quad \bar{f}_{slip/MS} = \frac{\|\mathbf{\Omega}_{slip/MS}^p\|}{\|\mathbf{\Omega}^p\|}, \quad (2.3)$$

where the norm of a second-order tensor \mathbf{A} (symmetric or not) is defined as $\|\mathbf{A}\| \equiv \sqrt{\mathbf{A} \cdot \mathbf{A}} = \sqrt{A_{ij}A_{ij}}$.

2.2. The single grain model with the yield surface of 2n-degree

In the classical Schmid multi-surface plasticity slip on the considered slip system is initiated if the resolved shear stress $\tau^r = \mathbf{m}^r \cdot \boldsymbol{\sigma} \cdot \mathbf{n}^r$ reaches the critical value τ_c^r being the material parameter. Instead of this formulation of the crystal plasticity with the single yield surface is used (Gambin, 1991). In view of this model the plastic deformation by crystallographic slip is activated when the following yield condition for the Cauchy stress $\boldsymbol{\sigma}$ is fulfilled

$$f(\boldsymbol{\sigma}) = \frac{1}{2n} \sum_{r=1}^M \left(\frac{\tau^r}{\tau_c^r} \right)^{2n} - m = 0, \quad (2.4)$$

where n is the positive exponent and m is the material parameter independent of the lattice orientation.

The rate of plastic deformation tensor due to crystallographic slip is specified with use of the associated flow rule

$$\mathbf{D}_{slip}^p = \dot{\lambda} \frac{\partial f(\boldsymbol{\sigma})}{\partial \boldsymbol{\sigma}} = \dot{\lambda} \sum_{r=1}^M \frac{1}{\tau_c^r} \left(\frac{\tau^r}{\tau_c^r} \right)^{2n-1} \frac{1}{2} (\mathbf{m}^r \otimes \mathbf{n}^r + \mathbf{n}^r \otimes \mathbf{m}^r). \quad (2.5)$$

Comparing the above flow rule with the kinematic relations (2.2) one finds

$$\boldsymbol{\Omega}_{slip}^p = \dot{\lambda} \sum_{r=1}^M \frac{1}{\tau_c^r} \left(\frac{\tau^r}{\tau_c^r} \right)^{2n-1} \frac{1}{2} (\mathbf{m}^r \otimes \mathbf{n}^r - \mathbf{n}^r \otimes \mathbf{m}^r). \quad (2.6)$$

In its mathematical structure this model is similar to the rate-dependent formulation of crystal plasticity (Asaro and Needleman, 1985), however, the reference velocity, which is the material parameter in the latter approach, is here replaced by the non-negative plastic multiplier $\dot{\lambda}$ obtained from the consistency condition $\dot{f} = 0$ for the yield surface (2.4). Plastic loading process ($\dot{\lambda} > 0$) is defined by $f = 0$ and $\dot{f} = 0$, while there is no rate of plastic flow ($\dot{\lambda} = 0$) when $f < 0$ or when $f = 0$ and $\dot{f} < 0$. The model was applied to study the crystallographic texture development and proved to give good results (Kowalczyk and Gambin, 2004). As in the case of the rate-dependent formulation the model enables to avoid known computational difficulties encountered when applying multisurface plasticity (Anand and Kothari, 1996), (Busso and Cailletaud, 2005).

Slip occurs by motion of dislocations that have to overcome both shortrange and long-range obstacles. Accumulation of dislocations make its further movement more and more difficult. This phenomenon is captured in the framework of crystal plasticity by the hardening rule for the critical resolved shear stress τ_c^r . In this study we use the formula proposed in (Asaro, 1983)

$$\dot{\tau}_c^r = \sum_{s=1}^M h^{rs} |\dot{\lambda}^s|, \quad (2.7)$$

where hardening matrix h^{rs} accounts for the latent and self-hardening by setting the parameter $q \neq 1$ in its specification $h^{rs} = h^{(s)}(q + (1-q)\delta^{rs})$ (no sum on s). For the function $h^{(s)}$ responsible for the self-hardening we assume the following equation (Anand and Kalidindi, 1994)

$$h^{(s)} = h_o \left| 1 - \frac{\tau_c^s}{\tau_{sat}^s} \right|^\beta \quad (2.8)$$

with the material parameters $\{h_o, \tau_{c0}^s, \tau_{sat}^s, \beta\}$ that have to be identified in the experiments, where τ_{c0}^s are

the initial values of critical resolved shear stresses τ_c^s .

2.3. Incorporation of micro-shear banding

In (Kowalczyk-Gajewska et al., 2005) two flow rules for micro-shear bands were considered. In both cases it was assumed that the yield condition (2.4) for the crystallographic slip mechanism was at the same time the yield condition for the micro-shear bands. This statement corresponds to the experimental observation that micro-shearing is never activated without even small contribution of crystallographic slip. Further, in the first specification of the model micro-shear banding was due to double shear and non-associated flow rule for \mathbf{D}_{MS}^p was formulated. To simplify the constitutive modelling we assume that the part of rate of plastic deformation \mathbf{D}_{MS}^p is associated with the yield surface described by Eq. (2.4). In such a case $f_{MS} + f_{slip} = 1$ and the total rate of plastic deformation tensor reads

$$\mathbf{D}^p = \frac{\mathbf{D}_{slip}^p}{1 - f_{MS}}, \quad 0 \leq f_{MS} < 1. \quad (2.9)$$

The effect of activity of micro-shear bands on the plastic yielding of the single grain is observed through the reduction of the hardening modules. Since the hardening rate depends on the increment of crystallographic slip (Eqs (2.5) and (2.7)), the higher contribution of micro-shear bands the higher is the reduction of the global strain hardening rate. In other words, increasing contribution of micro-shear banding will cause reduction of the current value of the yield stress comparing to the model without micro-shear band mechanism of plastic deformation.

For the plastic spin $\boldsymbol{\Omega}_{MS}^p$ we follow the concept discussed in (Dafalias, 1984). It specifies the plastic spin as proportional to the non-coaxiality factor between corresponding the plastic rate of deformation tensor (here \mathbf{D}_{MS}^p) and the Cauchy stress tensor. The scalar proportionality coefficient is in general an isotropic function of stress tensor and the orientational variables describing the material anisotropy. In the cited paper this function was identified in the experiments. In our model, instead of specifying this function we specify the function \bar{f}_{MS} . Applying the notation (2.3) corresponding relation may be written in the form

$$\boldsymbol{\Omega}_{MS}^p = \bar{f}_{MS} \|\boldsymbol{\Omega}^p\| \frac{\mathbf{D}_{MS}^p \boldsymbol{\sigma} - \boldsymbol{\sigma} \mathbf{D}_{MS}^p}{\|\mathbf{D}_{MS}^p \boldsymbol{\sigma} - \boldsymbol{\sigma} \mathbf{D}_{MS}^p\|} \quad (2.10)$$

Using the definition (2.3)₂ and Eq. (2.6) the value of $\|\boldsymbol{\Omega}^p\|$ can be related to $\dot{\lambda}$ and \bar{f}_{MS} . The function \bar{f}_{MS} is in the simplified model the additional unknown for

which some constitutive equation should be supplied. In the calculations we have studied two possibilities

$$\bar{f}_{MS} = 0, \text{ or } \bar{f}_{MS} = f_{MS} \quad (2.11)$$

where only the f_{MS} that describes the instantaneous contribution of the shear banding in the total rate of plastic deformation remains to be defined.

Let this function be defined by the following relation:

$$f_{MS}(\xi) = \frac{f_{MS}^\infty}{1 + \exp(a - b\xi)}. \quad (2.12)$$

In order to incorporate the effect of the type of strain path and its change suggested by experimental observations invoked in Sec. 1 we propose the following specification of the invariant ξ

$$\xi = \sqrt{\frac{3}{2}} \varepsilon_{eq}^p (1 - \alpha |\cos 3\theta|), \quad 0 \leq \alpha \leq 1, \quad (2.13)$$

where

$$\dot{\varepsilon}_{eq}^p = \sqrt{\frac{2}{3} \mathbf{D}^p \cdot \mathbf{D}^p}, \quad |\cos 3\theta| = 3 \sqrt{6} |\text{dct}(\mathbf{D}^p / \|\mathbf{D}^p\|)|. \quad (2.14)$$

The proposed form of ξ is relatively simple while in the same time, with use of $|\cos 3\theta|$, it accounts for experimentally observed more frequent appearance of micro-shear banding in the plane strain than in the simple compression (see Fig. 1b). The coefficient α is an additional material parameter that describes to what extent the scheme of strain path influences on the contribution of micro-shear banding into the rate of plastic deformation for the considered material. Note that in some cases rapid increase of the contribution of microshear bands can be observed when the scheme of the proportional strain path is changed in the course of deformation (see Fig 1a).

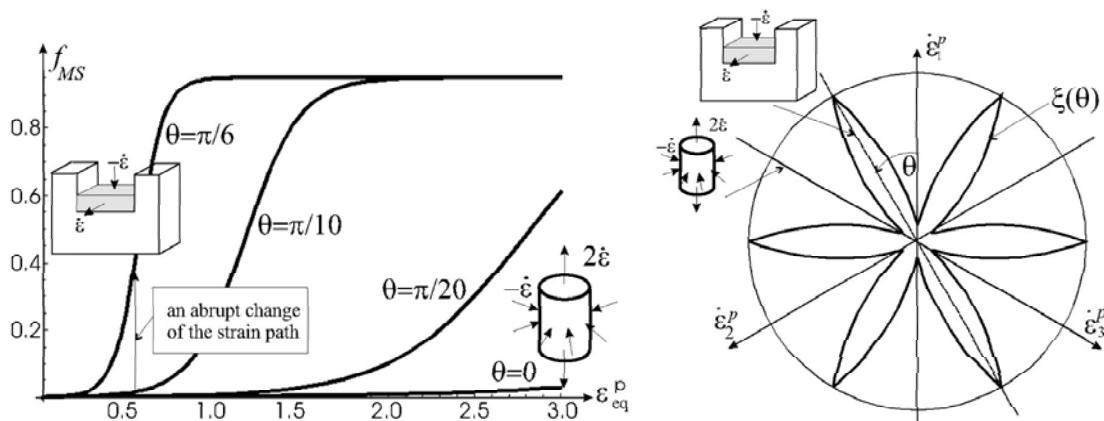


Fig. 1. The variation of f_{MS} representing contribution of micro-shear band in the plastic strain rate in the course of the deformation process (left) and the variation of ξ for the constant value of the equivalent plastic strain (right). Different proportional strain paths are described by the angle θ

Let us now discuss how the developed constitutive model predicts the lattice reorientation during the process of large plastic deformations. We compare the results obtained for the classical model that does not incorporate the microshear bands as additional mechanism and two models specified by (2.11). It should be expected that when the micro-shear banding is added the lattice orientation stabilizes earlier than for the model with pure crystallographic slip mechanism of plastic deformation. The difference between the models specified by (2.11) is also expected. In the first case the orientation path should be preserved although the distance passed by the pole throughout the process should be shorter comparing to the classical crystal plasticity model. In the second case,

at the moment when the contribution of micro-shear banding becomes to be noticeable the orientation path should start to deviate from the path predicted by the classical model. The observation that in the presence of micro-shear bands the developed crystallographic texture is different (Paul et al., 2003, 1996; Stalony-Dobrzanski and Bochniak, 2005) may be explained by the localized character of plastic deformation. Outside the zones of micro-shear banding the rate of plastic deformation is much smaller than the averaged rate of plastic deformation in the whole volume element. One important remark should be made at this point. Although Eq. (2.9) suggests that the current direction of the strain rate tensor is not affected by the microshear banding, such effect is

included within the model. Since the process of lattice reorientation changes when micro-shear banding is taken into account, different slip systems are being activated in the course of deformation process and consequently the direction of the current plastic strain rate tensor is changing.

3. Numerical simulations

3.1. Identification of the model

For the developed model different deformation paths are studied. The analysis is performed at the material

point on the level of a polycrystalline sample. As the representative volume element (RVE) for this macroscopic material point, the aggregate composed of 1000 grains with initially random distribution of lattice orientations is assumed (see Fig. 2). As a micro-macro transition rule the Taylor hypothesis is applied assuming that the velocity gradient \mathbf{L}^g in every grain is the same and equal to the macroscopic velocity gradient \mathbf{L} . The macroscopic stress and plastic dissipation are calculated as follows

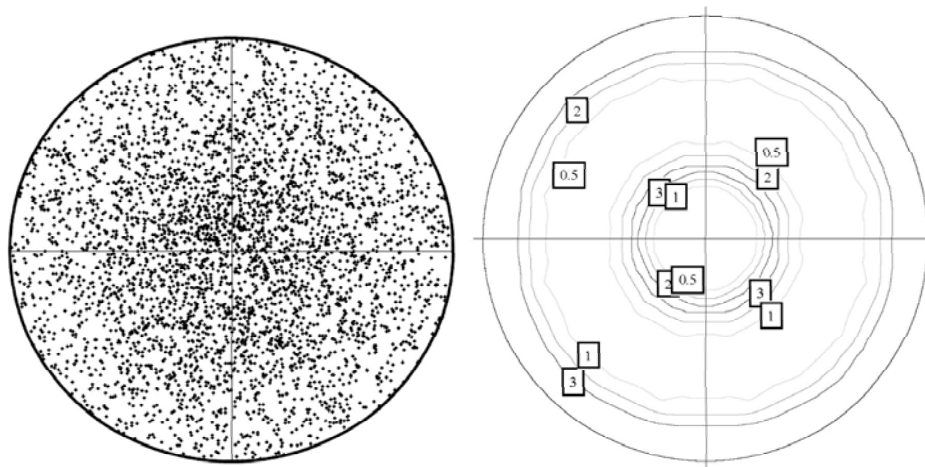


Fig. 2. The pole figure $\{111\}$ (stereographic projection) for the aggregate of 1000 grains: a) initial, b) final for the simple compression (logarithmic axial strain $\varepsilon_{11} = -1.0$), lines are multiples of random distribution

$$\Sigma = \sum_{g=1}^N v^g \sigma^g, \quad \dot{W}^p = \Sigma \cdot \mathbf{D}^p \Rightarrow W^p = \int_0^t \dot{W}^p dt, \quad (3.15)$$

where v^g is the volume fraction of grains with the orientation g in RVE. The value of the phenomenological function f_{MS} (2.12) is the same in every grain of RVE predicting the same contribution of micro-shear bands into the rate of plastic deformation throughout the aggregate. Let us stress that it is the consequence of both: the Taylor hypothesis and neglecting elasticity.

Note that in reality strains vary within the grain aggregate and within the single grain. The presented model of single grain may be applied for any micro-macro transition scheme used recently in numerical simulations of the behavior of polycrystals. In particular, using the self-consistent transition scheme one may account for the heterogeneity of deformation from grain to grain while using the FE-model of polycrystalline aggregate it is possible to observe also the deformation heterogeneity within the single grain. In these two cases analyzing the value

of f_{MS} function across the considered volume element it is possible to study space distribution of micro-shear banding activity. This kind of more complicated and sophisticated aggregate modelling is under development and results will be presented in the future. However, the Taylor model has an appealing virtue of simplicity and it proved to give results of first-order agreement with experiments in many analysis of single-phase fcc materials (Kalidindi and Anand, 1994), especially concerning the texture evolution and the polycrystal response for large strain regime. Therefore, it is a natural first step for studying the prediction ability of the proposed model. However, it should be underlined that the model accounts only for the reduction of global hardening rate due to micro-shear banding and its influence on the texture image without providing the information about its geometry and space distribution.

The identification of the material parameters has been performed with use of experimental data for the polycrystalline copper reported in (Kalidindi and Anand, 1994) and (Anand, 2004). We have assumed that the

micro-shear banding has a negligible contribution to the rate of plastic deformation in the case of simple compression (parameter $\alpha = 0.95$ has been prescribed) what is shown by the line presenting the evolution of f_{MS} . Therefore, similarly as in (Kalidindi and Anand, 1994),

the material parameters for the hardening rule for slip mechanism have been identified by fitting the predicted stress-strain curve to the experimental data for simple compression (see Fig. 3). We have prescribed the following velocity gradient in the specimen axes $\{e_k\}$

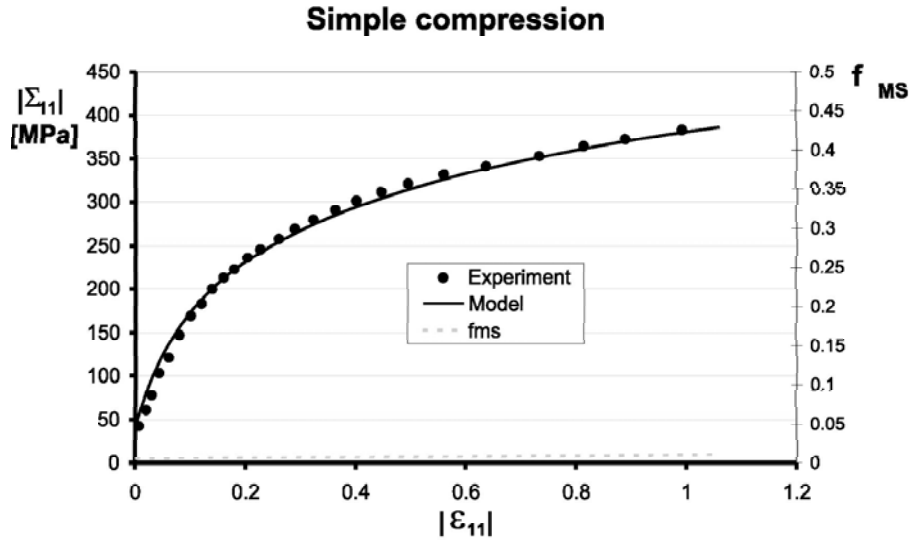


Fig. 3. Prediction of axial stress versus logarithmic axial strain in simple compression. Experimental data are approximated from (Anand, 2004)

$$L_{ij} = \frac{\dot{\epsilon}}{\sqrt{6}} \begin{bmatrix} -2 & 0 & 0 \\ 0 & 1 & 0 \\ 0 & 0 & 1 \end{bmatrix}, \quad \xi = \dot{\epsilon}t(1 - \alpha)$$

The following set of parameters has been obtained $n = 20$, $\tau_{c0} = 14$ MPa, $h_0 = 232.75$ MPa, $\tau_{sat} = 138.6$ MPa, $q = 1.4$, $\beta = 2.5$.

The texture development has been also studied. The resulting texture for the process is presented in Fig. 2b in the form of standard pole figure $\{111\}$. It quite successfully reproduces the experimental pole figure reported in (Kalidindi and Anand, 1994).

The parameters for the f_{MS} function have been identified by simulating the behavior of the considered polycrystalline element for plane strain compression. The following velocity gradient has been assumed

$$L_{ij} = \frac{\dot{\epsilon}}{\sqrt{2}} \begin{bmatrix} 1 & 0 & 0 \\ 0 & 0 & 0 \\ 0 & 0 & -1 \end{bmatrix}, \quad \xi = \dot{\epsilon}t$$

Two specifications (2.11) of the \bar{f}_{MS} have been applied and the following two sets of material parameters have been identified

$$\bar{f}_{MS} = f_{MS} \Rightarrow \alpha = 0.95, \quad f_{MS}^{\infty} = 0.85, \quad \alpha = 5.0, \quad b = 9.62,$$

$$\bar{f}_{MS} = 0 \Rightarrow \alpha = 0.95, \quad f_{MS}^{\infty} = 0.82, \quad \alpha = 5.0, \quad b = 9.62.$$

Fig. 4 indicates that with use of the proposed model it is possible to conform well at the same time to the strain-stress curves for simple compression and plane strain compression. Such concordance is difficult to achieve with use of classical crystal plasticity as seen in (Anand, 2004). The difference between the classical crystal plasticity and the developed model relies on the reduction of hardening rate due to the development of micro-shear bands described by means of the phenomenological function f_{MS} . When the value of this contribution function is high enough curves begin to deviate what enables to obtain the reduction of the stress level.

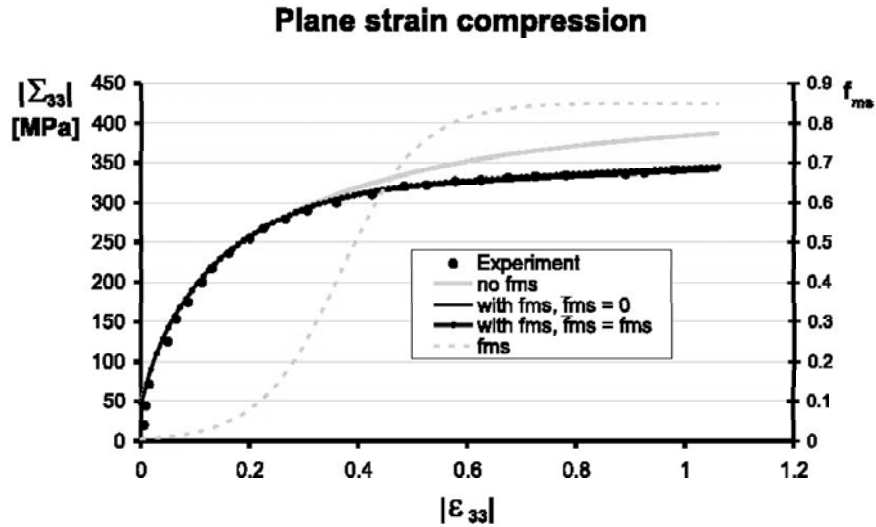


Fig. 4. Prediction of axial stress versus logarithmic axial strain in plane strain compression. Experimental data are approximated from (Anand, 2004)

In Fig. 5 the final crystallographic texture is presented for three models. One may observe that the qualitative agreement with the experimental results reported in (Anand, 2004) and (Kalidindi and Anand, 1994) has

been obtained for all models, though the best one seems to be the result for the model accounting for micro-shear bands and assuming $\bar{f}_{MS} = f_{MS}$.

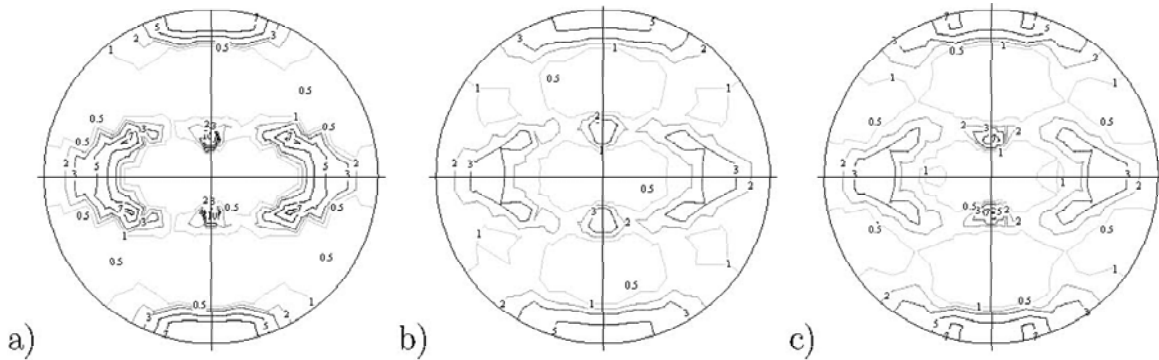


Fig. 5. The final pole figure {111} (stereographic projection) for the aggregate of 1000 grains for the plain strain compression (the logarithmic strain $|\epsilon_{33}| = 1 : 0$): a) model without f_{MS} , b) model with f_{MS} and $\bar{f}_{MS} = 0$, c) model with f_{MS} and $\bar{f}_{MS} = f_{MS}$; lines are multiples of random distribution

To close this point the prediction of the plastic work is analyzed. In Fig. 6 the variation of plastic work versus the equivalent plastic strain is presented for simple compression and plane strain compression. There is a difference between the magnitude of plastic work for

the same level of accumulated plastic strain for these two processes. The reason is the Tresca-like shape of the polycrystalline yield surface. Additional reduction of plastic work is observed when the effect of shear banding is taken into account.

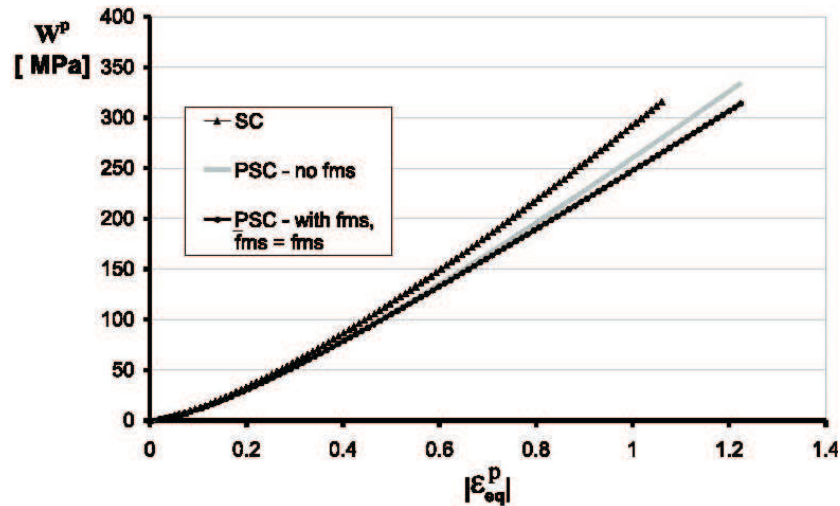


Fig. 6. Prediction of plastic work versus equivalent plastic strain for simple compression (SC) and plane strain compression (PSC)

3.2. Simulations of the processes with non-proportional deformation path – simple shear

Now, let us pass to the simulations of the process with non-monotonic deformation path. We will analyze the results obtained for simple shear. In this case the velocity gradient remains constant

$$L_{ij} = \dot{\gamma} \begin{bmatrix} 1 & -1 & 0 \\ 0 & 0 & 0 \\ 0 & 0 & 0 \end{bmatrix}, \quad \xi = \frac{\dot{\gamma}t}{\sqrt{2}}$$

though, the principal directions of the logarithmic strain tensor change during the process. It can be noticed that the value of $|\cos 3\theta| = 0$ in Eq. (2.13), similarly as in the case of the plane strain compression.

The curve of the macroscopic shear stress versus amount of shear is well predicted by the applied models, Fig. 7, though discrepancies between experimental results and numerical simulations are visible especially at the first stage of the process. Let us remind that the elastic stretches are neglected what may be one of the reasons. The texture development has also been studied. The results are presented in Fig. 8. They are qualitatively similar to the textures observed in experiments.

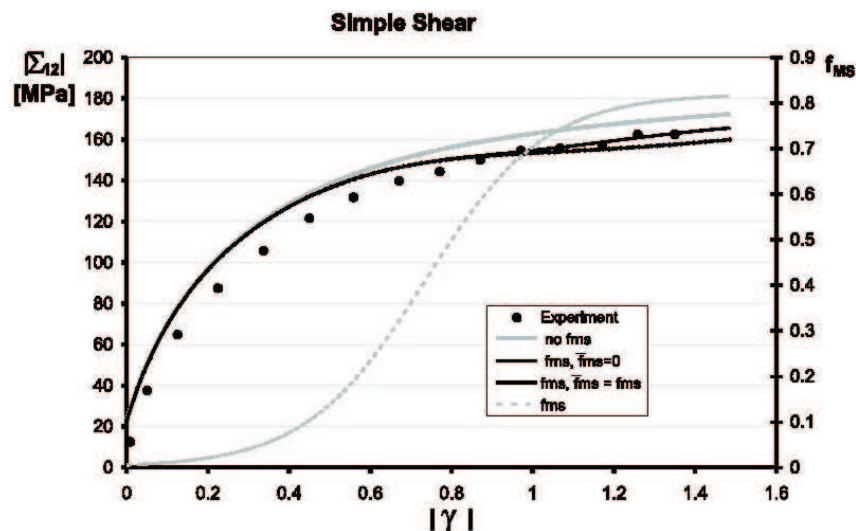


Fig. 7. Prediction of shear stress versus amount of shear in simple shear process. Experimental data are approximated from Anand (2004)

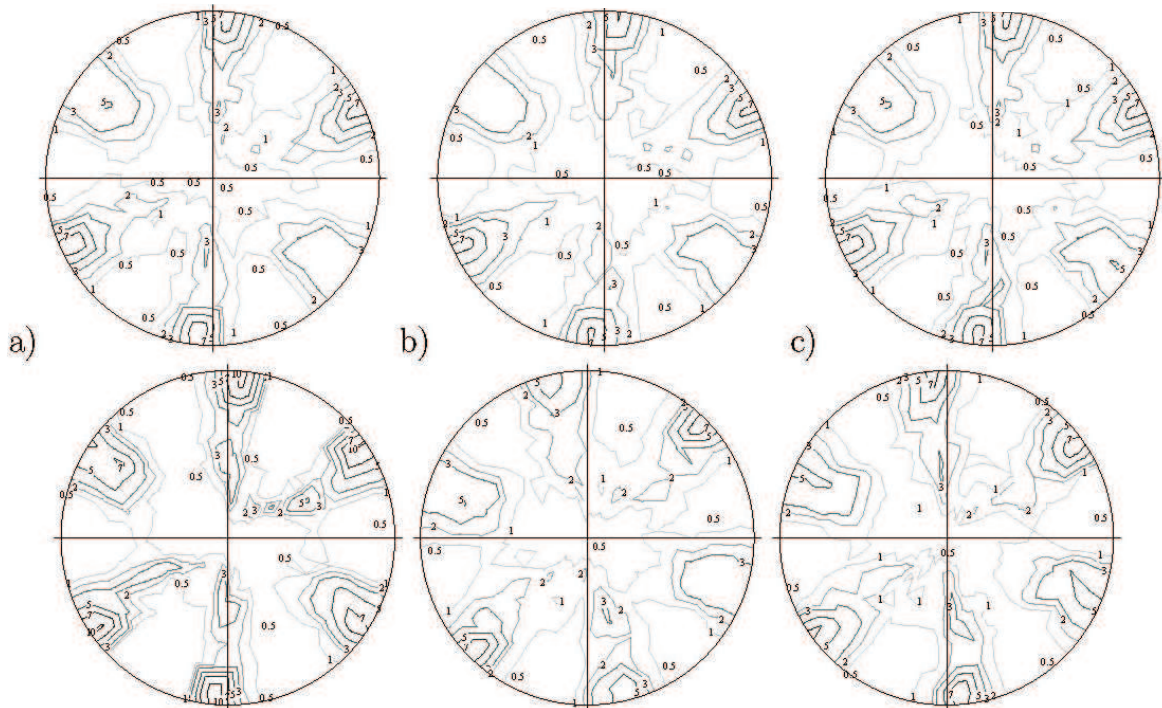


Fig. 8. The pole figures $\{111\}$ (stereographic projection) for the aggregate of 1000 grains for the simple shear, the upper row $|\gamma| = 0.7$, the lower row $|\gamma| = 1.4$: a) model without f_{MS} , b) model with f_{MS} and $\bar{f}_{MS} = 0$, c) model with f_{MS} and $\bar{f}_{MS} = f_{MS}$; lines are multiples of random distribution

The simple shear process enables to analyze the influence of the description of the plastic spin on the polycrystalline behavior. In the case of the classical crystal plasticity we observe quite sharp textures that are typical for the Taylor model. The textures measured experimentally are not so strong (compare (Anand, 2004)). Addition of the effect of shear banding causes that the texture image is not so sharp. An assumption that micro-shear banding does not contribute to the plastic spin causes that as the f_{MS} increases the plastic spin tends to zero. Consequently the elastic spin tends to be equal to the material spin. Due to the Taylor assumption it leads to the equal lattice reorientation in all grains manifested by the rigid rotation of the texture image (compare upper and lower row in Fig. 8b). The impediment of the texture development is also visible in Fig. 5 for the plane strain compression. In the case of $\bar{f}_{MS} = f_{MS}$ with the increasing contribution of shear banding the plastic spin begins to follow the rule (2.10) and the developed texture is different, Fig. 8c. The noticeable rigid rotation is smaller than in the previous case.

4. Conclusions

The crystal plasticity model accounting for the effect of micro-shear banding with use of the phenomenological function f_{MS} has been presented. The developed

approach enables to describe different behavior of the material in terms of the reduction of strain hardening depending on the loading scheme. According to the model the evolution of micro-shear banding impedes or changes texture evolution what agrees with the tendency observed in experiments. In the separate paper (Kowalczyk-Gajewska et al., 2007) the presented model has been applied for the prediction of material response in cyclic processes. The model predictions were in qualitative agreement with the reported experimental observations.

The proposed model of a single crystal considered as a single grain embedded in polycrystalline aggregate accounting for micro-shear banding can be applied for any micro-macro transition scheme used recently in numerical simulations of the behavior of polycrystals. The presented model needs further research, in particular there is a need for a verification of model predictions concerning the material response and the texture evolution with respect to the experimental results for different monotonic strain paths and those involving the strain path changes. From the modelling point of view the addition of twinning mechanism and more refined scale transition scheme should be considered.

Acknowledgements

Most of the results reported in the paper was obtained in the

framework of the research project No. PBZ-KBN-102/T08/2003 supported by the Ministry of Science and Higher Education of Poland.

REFERENCES

- [1] F. Adcock, The internal mechanism of cold-work and recrystallization in Cupro-Nickel. *J. Institute of Metals* **27**, 73–92 (1922).
- [2] L. Anand, Single-crystal elasto-viscoplasticity: application to texture evolution in polycrystalline metals at large strain. *Comput. Methods Appl. Mech. Engrg.* **193**, 5359–5383 (2004).
- [3] L. Anand, S. R. Kalidindi, The process of shear band formation in plane strain compression of fcc metals: Effects of crystallographic texture. *Mech. Mater.* **17**, 223–243 (1994).
- [4] L. Anand, M. Kothari, A computational procedure for rate independent crystal plasticity. *J. Mech. Phys. Solids* **44** (4), 525–558 (1996).
- [5] R. J. Asaro, Crystal plasticity. *J. Applied Mechanics* **50**, 921–934 (1983).
- [6] R. J. Asaro, A. Needleman, Textured development and strain hardening in rate dependent polycrystals. *Acta metall.* **33** (6), 923–953 (1985).
- [7] E. P. Busso, G. Cailletaud, On the selection of active slip systems in crystal plasticity. *Int. J. Plasticity* **21**, 2212–2231 (2005).
- [8] J. L. F. Coffin, The stability of metals under cyclic plastic strain. *J. Basic Eng.* **82D**, 671–682 (1960).
- [9] Y. F. Dafalias, The plastic spin concept and a simple illustration of its role in finite plastic transformations. *Mech. Mater.* **3**, 223–233 (1984).
- [10] S. D. Dugdale, Stress-strain cycles of large amplitude. *J. Mech. Phys. Solids* **7**, 135–142 (1959).
- [11] B. J. Duggan, M. Hatherly, W. B. Hutchinson, P. T. Wakefield, Deformation structures and textures in cold-rolled 70:30 brass. *Metal. Sci.* **12**, 343–351 (1978).
- [12] J. D. Embury, A. Korbel, V. S. Raghunathan, J. Rys, Shear band formation in cold-rolled Cu-65%Al single crystals. *Acta Metall.* **32**, 1883–1894 (1984).
- [13] W. Gambin, Crystal plasticity based on yield surface with rounded-off corners. *ZAMM* **71** (4), T265–T268 (1991).
- [14] S. V. Harren, H. E. Deve, R. J. Asaro, Shear band formation in plain strain compression. *Acta Metall.* **36**, 2435–2480 (1988).
- [15] M. Hatherly, A. S. Malin, Shear band in deformed metals. *Scripta Metall.* **18**, 449–454 (1984).
- [16] S. R. Kalidindi, L. Anand, Macroscopic shape change and evolution of crystallographic texture in pre-textured fcc metals. *J. Mech. Phys. Solids* **42**, 459–490 (1994).
- [17] L. X. Kong, L. Lin, P. D. Hodgson, Material properties under drawing and extrusion with cyclic torsion. *Mater. Sci. Engrg. A* **A308**, 209–215 (2001).
- [18] A. Korbel, W. Bochniak, Refinement and control of metals structure elements by plastic deformation. *Scripta Metar.* **51**, 755–759 (2004).
- [19] A. Korbel, J. D. Embury, M. Hatherly, P. L. Martin, H. W. Erbsloh, Microstructural aspects of strain localization in Al-Mg alloys. *Acta Metall.* **34**, 1999–2009 (1986).
- [20] A. Korbel, P. L. Martin, Microstructural events of macroscopic strain localization in prestrain tensile specimens. *Acta Metall.* **36**, 2575 (1988).
- [21] K. Kowalczyk, W. Gambin, Model of plastic anisotropy evolution with texture-dependent yield surface. *Int. J. Plasticity* **20**, 19–54 (2004).
- [22] K. Kowalczyk-Gajewska, W. Gambin, R. B. Pecherski, J. Ostrowska-Maciejewska, Modelling of crystallographic texture development in metals accounting for micro-shear banding. *Arch. Metall. Mater.* **50**, 575–593 (2005).
- [23] K. Kowalczyk-Gajewska, Z. Mróz, R. B. Pecherski, Micromechanical modelling of polycrystalline materials under non-proportional deformation paths. *Arch. Metall. Mater.* **52**, 181–192 (2007).
- [24] A. A. S. Mohammed, E. A. El-Danaf, A. A. Radwan, A criterion for shear banding localization in polycrystalline fcc metals and alloys and critical working conditions for different microstructural variables. *J. Mater. Proc. Technol.* **186**, 14–21 (2007).
- [25] Z. Mróz, K. Kowalczyk-Gajewska, J. Maciejewski, R. B. Pecherski, Tensile or compressive plastic deformation assisted by cyclic torsion. *Arch. Mech.* **58**, 497–527 (2006).
- [26] Z. Mróz, R. B. Pecherski, Metal forming processes conditioned by cyclic loading. a new challenge for the theory of plasticity. In: Kowalewski, T., Gutkowski, W. (Eds.), *Proc. ICTAM 2004*. Springer.
- [27] H. Paul, J. H. Driver, C. Maurice, Z. Jasienski, Shear band microtexture formation in twinned face centered cubic single crystals. *Mater. Sci. Engrg. A* **359**, 178–191 (2003).
- [28] H. Paul, Z. Jasienski, A. Piatkowski, A. Litwora, A. Pawelek, Crystallographic nature of shear bands in polycrystalline copper. *Arch. Metall.* **41**, 337–353 (1996).
- [29] R. B. Pecherski, Modelling of large plastic deformation based on the mechanism of micro-shear banding. *Physical foundations and theoretical description in plane strain. Arch. Mech.* **44**, 563–584 (1992).
- [30] R. B. Pecherski, Macroscopic measure of the rate deformation produced by micro-shear banding. *Arch. Mech.* **49**, 385–401 (1997).
- [31] R. B. Pecherski, Continuum mechanics description of plastic flow produced by micro-shear banding. *Technische Mechanik* **18**, 563–584 (1998a).
- [32] R. B. Pecherski, Macroscopic effects of micro-shear banding in plasticity of metals. *Acta Mechanica* **131**, 203–224 (1998b).
- [33] J. G. Sevillano, P. van Houtte, E.

- A e r n o u d t, Large strain work hardening and textures. *Progress in Material Science* **25**, 69–412 (1981).
- [34] F. S t a l o n y - D o b r z a n s k i, W. B o c h n i a k, Role of shear bands in forming the texture image of deformed copper alloy. *Arch. Metall. Mater.* **50**, 1089–1102 (2005).
- [35] W. Y. Y e u n g, B. J. D u g g a n, On the plastic strain carried by shear bands in cold-rolled α -brass. *Scripta Metall.* **21**, 485–490 (1987).

Received: 20 March 2009.